Developmental Cell
Article

Mechanotransduction, PROX1, and FOXC2 Cooperate to Control Connexin37 and Calcineurin during Lymphatic-Valve Formation

Amélie Sabine,[1,2] Yan Agalarov,[1,2] Hélène Maby-El Hajjami,[1,2] Muriel Jaquet,[1,2] René Hägerling,[3] Cathrin Pollmann,[3] Damien Bebber,[1,2] Anna Pfenniger,[5] Naoyuki Miura,[6] Olivier Dormond,[7] Jean-Marie Calmes,[7] Ralf H. Adams,[3,4] Taija Mäkinen,[8] Friedemann Kiefer,[3] Brenda R. Kwak,[5] and Tatiana V. Petrova[1,2,*]

[1]Division of Experimental Oncology, Multidisciplinary Oncology Center, University Hospital of Lausanne, and Department of Biochemistry, University of Lausanne, 1066 Epalinges, Switzerland
[2]École Polytechnique Fédérale de Lausanne (EPFL), Swiss Institute for Experimental Cancer Research (ISREC), 1015 Lausanne, Switzerland
[3]Max Planck Institute for Molecular Biomedicine, 48149 Münster, Germany
[4]University of Münster, Faculty of Medicine, 48149 Münster, Germany
[5]Department of Pathology and Immunology, and Department of Internal Medicine – Cardiology, University of Geneva, CH-1211 Geneva, Switzerland
[6]Hamamatsu University School of Medicine, 431-3192 Hamamatsu, Japan
[7]Department of Visceral Surgery, University Hospital of Lausanne, 1011 Lausanne, Switzerland
[8]Cancer Research UK London Research Institute, 44 Lincoln's Inn Fields, WC2A 3LY London, UK
*Correspondence: tatiana.petrova@unil.ch
DOI 10.1016/j.devcel.2011.12.020

SUMMARY

Lymphatic valves are essential for efficient lymphatic transport, but the mechanisms of early lymphatic-valve morphogenesis and the role of biomechanical forces are not well understood. We found that the transcription factors PROX1 and FOXC2, highly expressed from the onset of valve formation, mediate segregation of lymphatic-valve-forming cells and cell mechanosensory responses to shear stress in vitro. Mechanistically, PROX1, FOXC2, and flow coordinately control expression of the gap junction protein connexin37 and activation of calcineurin/NFAT signaling. Connexin37 and calcineurin are required for the assembly and delimitation of lymphatic valve territory during development and for its postnatal maintenance. We propose a model in which regionally increased levels/activation states of transcription factors cooperate with mechanotransduction to induce a discrete cell-signaling pattern and morphogenetic event, such as formation of lymphatic valves. Our results also provide molecular insights into the role of endothelial cell identity in the regulation of vascular mechanotransduction.

INTRODUCTION

Lymphatic vasculature contains two distinct functional compartments: lymphatic capillaries, important for the uptake of interstitial fluid, and collecting lymphatic vessels, which transport lymph toward lymph nodes. Intraluminal lymphatic valves are the hallmark of the collecting-lymphatic-vessel phenotype. They are composed of two semilunar leaflets, covered on both sides by a specialized endothelium tightly anchored to an extracellular matrix (ECM) core. Lymphatic valves prevent lymph backflow: high hydrostatic pressure in the upstream duct opens the valve and enables forward flow. In contrast, pressure from the opposite direction pushes the two valve leaflets together and thereby stops reverse lymph flow. Lymphatic-valve dysfunction underlies some forms of human hereditary lymphedema, and it is one of the likely causes of secondary lymphedema, which affects up to 30% of breast cancer patients following the resection of axillary lymph nodes (Rockson, 2008).

Few regulators of lymphatic-valve formation have been identified to date. Loss of transcription factor Foxc2 and EphB tyrosine kinase ligand ephrinB2 prevents formation of lymphatic valves, whereas inactivation of integrin α9 or its ECM ligand FN-EIIIA affects the elongation of lymphatic-valve leaflets, leading to nonfunctional valves (Bazigou et al., 2009; Mäkinen et al., 2005; Norrmén et al., 2009; Petrova et al., 2004). FOXC2-bound enhancers from lymphatic endothelial cells (LECs) are enriched in binding sites for nuclear factor of activated T cells (NFAT) transcription factors, and pharmacological inhibition of calcineurin, an upstream regulator of NFAT activation, affects lymphatic-valve formation (Norrmén et al., 2009). Despite this knowledge, the processes during early stages of lymphatic-valve development are still not well understood. The transcription factor Prox1, required for the establishment of lymphatic endothelial cell identity (Wigle and Oliver, 1999), and Foxc2 are upregulated, coexpressed, and required from the onset of lymphatic- or lymphovenous-valve formation (Bazigou et al., 2009; Norrmén et al., 2009; Srinivasan and Oliver, 2011). Here, we investigated how early lymphatic-valve morphogenesis is regulated via the interplay of these transcription factors, mechanical stimulation by lymph flow, and downstream target genes and pathways, such as connexins and calcineurin signaling.

RESULTS

Steps of Embryonic Lymphatic-Valve Formation

E15.5 mesenteric lymphatic endothelial cells form a network of maturing collecting vessels (Norrmén et al., 2009). Formation of lymphatic valves is initiated around E16.0, and upregulation of Prox1, followed by a less pronounced upregulation of Foxc2 shortly afterward, is the first sign of it (Figure 1A; Bazigou et al., 2009; Norrmén et al., 2009). Clusters of Prox1^{high} lymphatic-valve-forming cells (LVCs) further coalesce and form a ring-like constriction composed of two to four rows of cells (Figure 1A). The absolute number of cells in the ring varies with the size of the lymphatic vessel (Figure S1A available online). Formation of a ring-like constriction is followed by downregulation of Foxc2 and Prox1 in cells that form the lymphangion (part of lymphatic vessel between two valves). These cells subsequently align and elongate in the direction of lymph flow. Interestingly, Foxc2 and Prox1 are localized asymmetrically in the regions immediately up- and downstream of LVCs: cells in the upstream region express lower levels of Foxc2 (Prox1^{high}/Foxc2^{low}), whereas cells located in the downstream region are Prox1^{low}/Foxc2^{high} (Figure 1A). Polarized distribution of Prox1 and Foxc2 may indicate that the direction of future lymphatic leaflet elongation is specified already at this stage.

During the next steps, a subset of LVCs is reoriented and protrudes into the lumen, starts to elongate, and forms valve leaflets (Figure 1B, top). These stages of lymphatic-valve formation are accompanied by deposition of ECM components, such as laminin α5, collagen IV, and FN-EIIIA, and increased expression of integrin α9, which anchors LVCs to the leaflet ECM matrix (Bazigou et al., 2009; Norrmén et al., 2009). Further deposition of ECM components during valve maturation results in the thickening of valve leaflets. In this study, we observed that LVC clusters start to produce laminin α5 early during valve initiation (Figure 1B, top).

Based on both previously published and new data, presented here, we suggest a four-step model for the formation of lymphatic valves, with each step identified by a double staining for Prox1 as an LVC marker and laminin α5 as an indicator of lymphatic-valve maturation. Valve formation initiates as isolated LVCs that first form a cluster of LVCs on one side of the collecting vessel (Stage 1, initiation). Then LVC cluster gives rise to a ring-like constriction (Stage 2, condensation). Next, increased deposition of laminin α5, together with invagination of LVCs into the lumen, indicates leaflet elongation (Stage 3, elongation). This is followed by valve maturation when two leaflets can be observed in association with a thick ECM core (Figure 1B, Stage 4, maturation).

Morphological and Molecular Changes during Valve Formation

We further characterized Prox1^{high} LVCs by staining for Pecam1, endothelial adherens junction protein VE-cadherin, F-actin, or β-catenin that anchors actin cytoskeleton to cell-cell junctions. Prox1^{high} LVCs displayed a cuboidal shape, perinuclear F-actin fibers, and β-catenin condensation (Figures 1C, S1B, and S1C). Surrounding lymphangion endothelial cells displayed more squamous cell characteristics and cortical actin cytoskeleton and β-catenin (Figures 1C, S1B, and S1C). Transition from squamous to cuboidal cell shape has also been observed at early stages of venous-valve development (Kampmeier and Brich, 1927) and in zebrafish heart-valve endocardial cells (Beis et al., 2005), suggesting that it is an important step in valve morphogenesis.

The lymphatic capillary marker LYVE-1 is downregulated in postnatal collecting vessels (Mäkinen et al., 2005). We observed that decrease in LYVE-1 is initiated already in early LVCs (Figure 1D). Receptors of lymphangiogenic factor Vegf-c, Vegfr-2, and Vegfr-3 were expressed in both LVCs and lymphangion cells (Figures 1E and 1F), but their coreceptor neuropilin-2 (Nrp2) was selectively decreased in LVCs and mature valves (Figures 1G and S1D).

Gap-Junction Protein Connexin37 and Calcineurin/NFAT Signaling Are Induced in Early Lymphatic-Valve-Forming Cells

The highly coordinated formation of ring-like constrictions by LVCs suggested that cell-cell communication is involved in this morphogenetic event. Therefore, we investigated the expression of vascular connexin37 (Cx37), Cx43, and Cx40, which form gap junctions and thus may control collective cell behavior (Wei et al., 2004). Cx37 was present in lymphatic vessels, as reported previously (Kanady et al., 2011). Importantly, we found that it is upregulated in LVCs to a level comparable to that in nearby arteries (Figure 1H). High Cx37 levels are observed shortly after Prox1 induction in a subset of LVCs. In contrast, Cx43 is highly expressed in embryonic lymphatic vessels, but is low in the early-stage LVCs in comparison to lymphangion endothelial cells (Figure 1I). Both Cx37 and Cx43 are expressed in the valves at later stages of lymphatic-valve development, while Cx40 is low in developing collecting lymphatic vessels (Figures S1E and S1F; F. le Noble, personal communication; Kanady et al., 2011).

The Ca^{2+}-dependent serine/threonine phosphatase calcineurin regulates nuclear translocation of NFAT transcription factors (Wu et al., 2007). It has been suggested that calcineurin-dependent activation of Nfatc1 plays a role in both lymphangiogenesis and formation of collecting lymphatic vessels in cooperation with Foxc2 (Kulkarni et al., 2009; Norrmén et al., 2009). We expanded this analysis by studying Nfatc1 localization in developing lymphatic valves. Nuclear Nfatc1 accumulated in LVCs, indicating activation of calcineurin signaling during early stages of lymphatic-valve formation (Figure 1J).

To summarize, LVCs acquire a distinct identity, and they undergo both morphological (cuboidal cell shape acquisition and cytoskeleton reorganization) and molecular transition (Figure 1K), raising questions about mechanisms and roles of these changes in lymphatic-valve formation.

Cx37 Is Essential for Assembly of the Ring-like Valve Territory In Vivo

We next studied the functional significance of increased Cx37 expression in LVCs. As reported previously (Kanady et al., 2011; Simon and McWhorter, 2002), blood vascular development and lymphatic endothelial differentiation were normal in *Cx37*$^{-/-}$ mice (Figures S2A and S2B), but most lymphatic vessels lacked lymphatic valves, resulting in a severely perturbed lymphatic drainage in adults (Figure S2C). We sought to investigate next the mechanisms underlying loss of valves in *Cx37*$^{-/-}$ mice. Prox1^{high}/Foxc2^{high} LVC clusters were detected

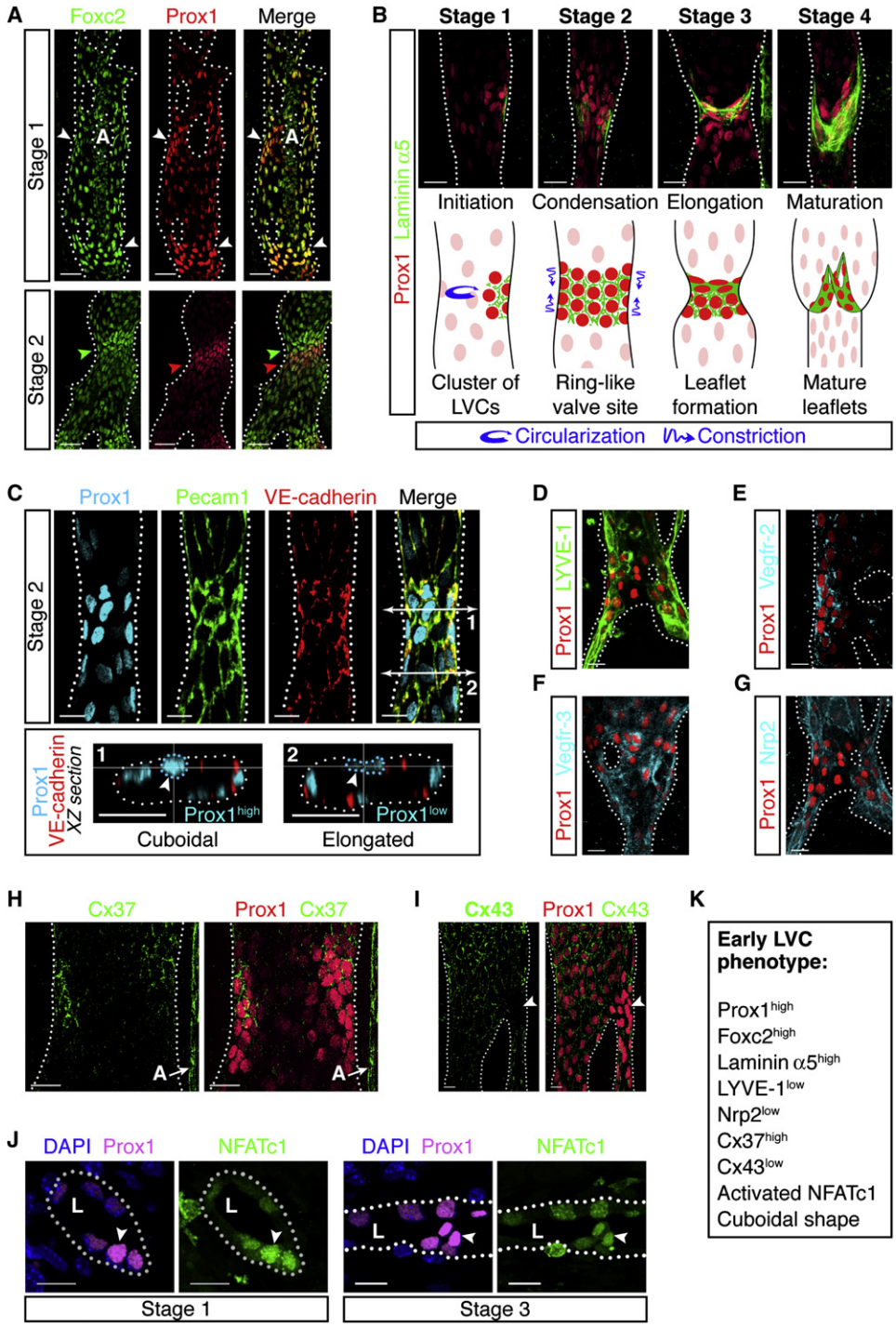

Figure 1. Characterization of Lymphatic Valve-Forming Cells

(A) Prox1 and Foxc2 expression at early stages of lymphatic valve morphogenesis. Top (Stage 1): Prox1 is upregulated during lymphatic valve initiation in a subset of LECs (arrowheads). A, artery. Bar, 100 μm. Bottom (Stage 2): ring-like constriction is formed by Prox1^{high}/Foxc2^{high} cells. Prox1^{high} ring is upstream of the valve (red arrowhead); Foxc2^{high} ring is downstream of the valve (green arrowhead). Bar, 50 μm. E16.0 and E17.0 mesenteric lymphatic vessels were stained for Prox1 (red) and Foxc2 (green).

(B) Stages of lymphatic-valve morphogenesis, showing staining of mesenteric lymphatic vessels for Prox1 (red) and laminin α5 (green) (Ringelmann et al., 1999). Bar, 20 μm.

(C) Valve-forming cells have a cuboidal shape. E16.5 mesenteric lymphatic vessels were stained for Prox1 (blue), Pecam1 (green), and VE-cadherin (red). Bottom: transverse sections of the vessel at the valve site (position 1) and in the lymphangion (position 2) obtained by *x-z* reconstructions from the confocal 3D picture. Arrowheads indicate shapes of nuclei in cuboidal and squamous lymphatic endothelial cells. Bar, 20 μm.

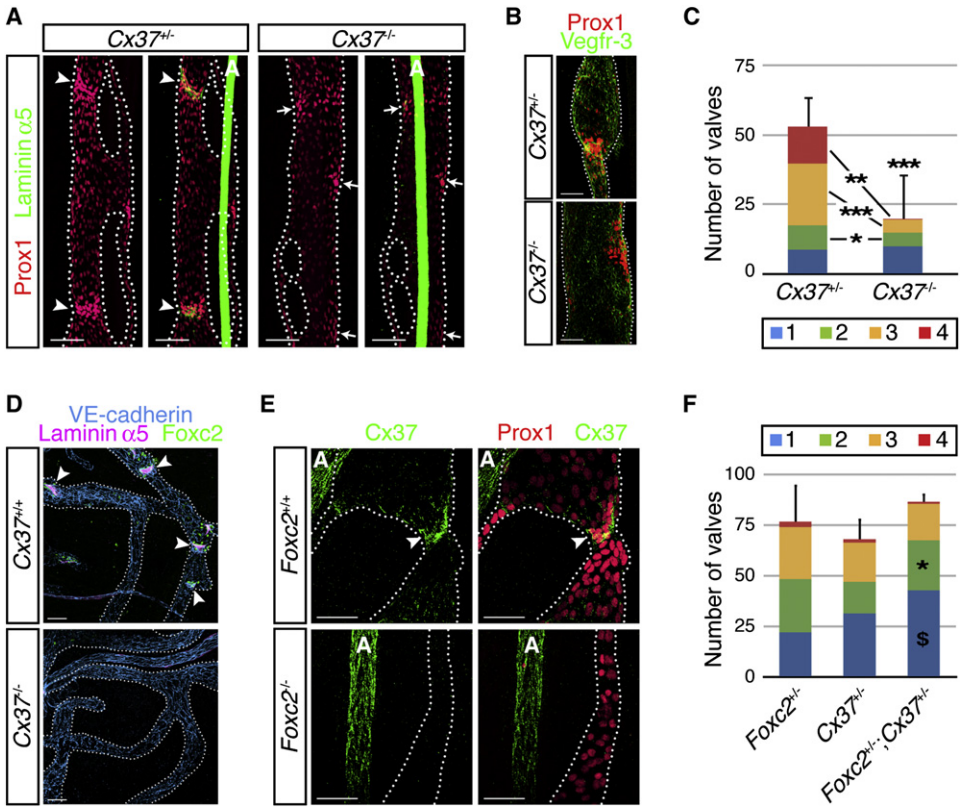

Figure 2. Cx37 Controls the Assembly of Circumferential Valve Territory

(A) Cx37 regulates lymphatic valve formation. E18.5 mesenteric vessels were stained for Prox1 (red) and laminin α5 (green). Arrowheads indicate mature valve sites, and arrows indicate immature valve sites. A, artery. Bar, 100 μm.

(B) Defective circumferential assembly of a valve site in *Cx37*$^{-/-}$ mice. E18.5 mesenteric vessels were stained for Vegfr-3 (green) and Prox1 (red). Bar, 80 μm.

(C) Quantification of mesenteric lymphatic valves in E18.5 embryos. *p < 0.05, **p < 0.005, ***p < 0.001, n = 10 embryos per genotype.

(D) The number of lymphatic valves is reduced in adult *Cx37*$^{-/-}$ mice. Diaphragms were stained for VE-cadherin (blue), Foxc2 (green), and laminin α5 (pink). Arrowheads indicate lymphatic valves. Bar, 70 μm.

(E) Cx37 expression is reduced in *Foxc2*$^{-/-}$ mice. E17.5 mesenteric vessels were stained for Prox1 (red) and Cx37 (green). Arrowheads indicate lymphatic valves. A, artery. Bar, 20 μm.

(F) Partial genetic interaction of *Foxc2* and *Cx37*. The number of valves at the initial assembly, stages 1 and 2, is increased in E18.5 *Foxc2*$^{+/-}$; *Cx37*$^{+/-}$ mice. *p < 0.005 versus *Cx37*$^{+/-}$, $^{\$}$p < 0.01 versus *Foxc2*$^{+/-}$, n = 3 embryos per genotype. Stages of valve development are as in Figure 1B.

See also Figure S2. All values are means ± SD.

in developing *Cx37*$^{-/-}$ collecting vessels (Figures 2A and S2D). However, LVCs failed to reorganize and form the ring-like constrictions observed in the control littermates (Figure 2B). The total number of valves was decreased and the majority was arrested at the initial stages of development (Figure 2C).

Valve formation was arrested and not simply delayed, as lymphatic valves were almost absent in all adult *Cx37*$^{-/-}$ tissues tested (Figures 2D and S2E). Unlike the case for prenatal lymphatic vessels, no isolated LVC clusters were observed in the adults, although a few fully mature valves were found (data not shown). These results suggest that LVC clusters are unstable in the absence of Cx37 and revert to the surrounding lymphangion phenotype. However, when a sufficient number of cells is present, further valve development appears to proceed normally.

Foxc2$^{-/-}$ embryos fail to develop lymphatic valves (Petrova et al., 2004), and Cx37 protein was almost completely absent

(D–G) LYVE-1 and Nrp2, but not Vegfr-2 and Vegfr-3, are decreased in lymphatic-valve-forming cells. E16.5 mesenteric vessels were stained for LYVE-1 (green), Vegfr-2, Vegfr-3, and Nrp2 (blue), and Prox1 (red). Bar, 20 μm.

(H) Cx37 is upregulated in lymphatic-valve-forming cells. E17.0 mesenteric lymphatic vessels were stained for Prox1 (red) and Cx37 (green). A, artery. Bar, 30 μm.

(I) Cx43 is downregulated in lymphatic-valve-forming cells. E17.0 mesenteric lymphatic vessels were stained for Prox1 (red) and Cx43 (green). Arrowheads indicate the lymphatic valve site. Bar, 20 μm.

(J) Calcineurin/NFAT pathway is activated in lymphatic-valve-forming cells. E17.5 sections were stained for DNA (blue), Prox1 (pink), and Nfatc1 (green). Left: valve at stage 1 (initiation); right, valve at stage 3 (elongation). L, lumen. Arrowheads indicate the lymphatic-valve-forming cell. Bar, 10 μm.

(K) Molecular characteristics of early lymphatic-valve-forming cells.

See also Figure S1.

in lymphatic vessels of *Foxc2*$^{-/-}$ mice, while its expression was unaltered in arteries, which also express Foxc2 (Figure 2E). Comparison of LECs isolated from *Foxc2*$^{-/-}$ with those from control wild-type mice demonstrated a significant reduction in *Cx37* mRNA (Figure S2F). These results, which are in agreement with Kanady et al. (2011), suggested that Cx37 is one of the downstream effectors of Foxc2 in the regulation of collecting-lymphatic-vessel phenotype and lymphatic-valve formation. To further validate this hypothesis, we analyzed lymphatic valves in double heterozygous *Foxc2*$^{+/-}$; *Cx37*$^{+/-}$ mice. We found that heterozygous loss of both *Foxc2* and *Cx37* reduced the proportion of mature valves (Figure 2F). However, unlike in *Cx37*$^{-/-}$ mice, the total number of valves was not affected, suggesting that additional mechanisms are involved.

Collectively, these data show that Cx37 regulates the transition from the early LVC cluster to a circumferential lymphatic valve territory. Loss of Cx37 prevents the formation of lymphatic valves and leads to a profoundly abnormal lymphatic drainage (Figures S2C and S2G).

Cell-Autonomous Calcineurin Signaling Controls Demarcation of the Lymphatic-Valve Territory

Pharmacological inhibition of calcineurin decreases lymphatic sprouting and maturation of collecting lymphatic vessels (Kulkarni et al., 2009; Norrmén et al., 2009). However, calcineurin is ubiquitously expressed, and it is not known whether the observed lymphatic vascular defects are cell-autonomous. To answer this question, we inactivated calcineurin regulatory subunit Cnb1 in different endothelial compartments after E12.5 (Figure S3A). Loss of *Cnb1* in blood endothelial cells (Figures S3B and S3C) did not affect patterning of blood or lymphatic vessels (Figures S3D–S3F), demonstrating that calcineurin is dispensable for late embryonic angiogenesis. Pan-endothelial *Cnb1* inactivation affected neither overall development, heart-valve formation, blood patterning, or lymphatic capillary patterning (Figures S3G–S3K). In contrast, loss of *Cnb1* resulted in poor demarcation of valve territory in developing collecting lymphatic vessels; i.e., a sharp boundary between Prox1^{low} and Prox1^{high} cells, observed in the control mice, was replaced by a large ring of Prox1^{high} cells, which failed to polarize and invaginate into the lumen (Figures 3A and 3B). A similar phenotype was observed when *Cnb1* was inactivated in lymphatic endothelial cells (Figures S3L and S3M). These data demonstrate that calcineurin signaling is required cell-autonomously for lymphatic-valve formation. In contrast, defects of lymphatic capillary sprouting observed after cyclosporin A treatment or in calcineurin Aβ-deficient mice (Kulkarni et al., 2009; Norrmén et al., 2009) may be due to the suppression of this pathway in nonendothelial cell type(s).

Calcineurin Signaling Is Necessary for the Maintenance of Lymphatic Valves

The calcineurin pathway remains active in adult lymphatic valves in both humans and mice (Figure 3C; data not shown). To study its role in valve maintenance, we inactivated *Cnb1* in the lymphatic vasculature of newborn pups and studied vessel morphology at postnatal day 7. Lymphatic valves of the control mice had elongated leaflets with well-formed laminin α5 ECM core (Figure 3D). In contrast, the number of valves and the ECM deposition were significantly reduced upon inactivation of *Cnb1* (Figures 3D and 3E), suggesting that postnatal loss of calcineurin signaling leads to valve-leaflet regression or degeneration. Furthermore, inactivation of calcineurin in fully mature lymphatic valves in adult mice resulted in significant shortening of the ECM core (Figures 3F and 3G). These results reveal a need for continuous calcineurin activation during the establishment and maintenance of lymphatic valves.

FOXC2 and PROX1 Control *Cx37* Expression and Calcineurin/NFAT Activation in Response to Flow

We next asked what mechanisms underlie enhanced expression of Cx37 and activation of calcineurin/NFAT in LVCs. Lymphangiogenic growth factor VEGF-C activates calcineurin/NFAT signaling in lymphatic endothelial cells (LECs) through VEGFR-2 (Norrmén et al., 2009). However, VEGF-C-elicited activation of calcineurin/NFAT was transient (Figures 4A and S4A), and VEGF-C decreased both FOXC2 and Cx37 proteins (Figures 4B and S4B). In addition, VEGF-C induced cell elongation (Figure 4C), whereas LVCs in vivo have a cuboidal shape (Figures 1C and S1B). These results suggest that VEGF-C is an unlikely candidate for the coordinate induction of Cx37 and calcineurin/NFAT activation in LVCs in vivo.

Reversing blood flow triggers heart-valve formation in zebrafish (Vermot et al., 2009) and lymphatic valves frequently form at vessel bifurcations (Kampmeier, 1928; Figure S1G), corresponding to areas of disturbed flow (Hahn and Schwartz, 2009). We next tested whether calcineurin/NFAT and Cx37 are induced in LECs by reversing flow, which we modeled by oscillatory fluid shear stress (OSS), based on the values reported for collecting lymphatic vessels (Zawieja, 2009). OSS induced a strong sustained accumulation of nuclear NFATc1 and expression of Cx37, which were abrogated by *PROX1* or *FOXC2* knockdown (Figures 4D–4F and S4C–S4G). In contrast, Cx43, which has been suggested to act together with Cx37 in lymphatic vasculature (Kanady et al., 2011), was repressed by OSS, similar to early LVCs in vivo (Figures 4G and S4G). The expression of Cx43 under static conditions was dependent on PROX1, whereas depletion of FOXC2 had little effect on *Cx43* mRNA (Figures S4C and S4G). Thus, it is possible that Cx43 cooperates with Cx37 at late stages of valve formation or that perhaps Cx43 is involved in nonendothelial cells. Most importantly, these results show that, unlike VEGF-C, flow coordinately induces *Cx37* and calcineurin/NFAT activation in a PROX1- and FOXC2-dependent manner.

Cx37 Acts Upstream of Calcineurin/NFAT Activation in Lymphatic Endothelial Cells

Connexin45 acts upstream of calcineurin during heart-valve formation (Kumai et al., 2000). We asked whether Cx37 contributes to the activation of calcineurin/NFAT in response to flow. Cx37 depletion significantly decreased calcineurin/NFAT activation by OSS (Figures 4H and S4F). While there was a uniform loss of nuclear NFATc1 upon depletion of FOXC2 or PROX1 (Figures 4D and 4E), loss of Cx37 resulted in a distinct phenotype, i.e., there were many isolated cells with high nuclear NFATc1. These results suggest that Cx37 acts downstream of PROX1 and FOXC2 to create a coordinated field of activated

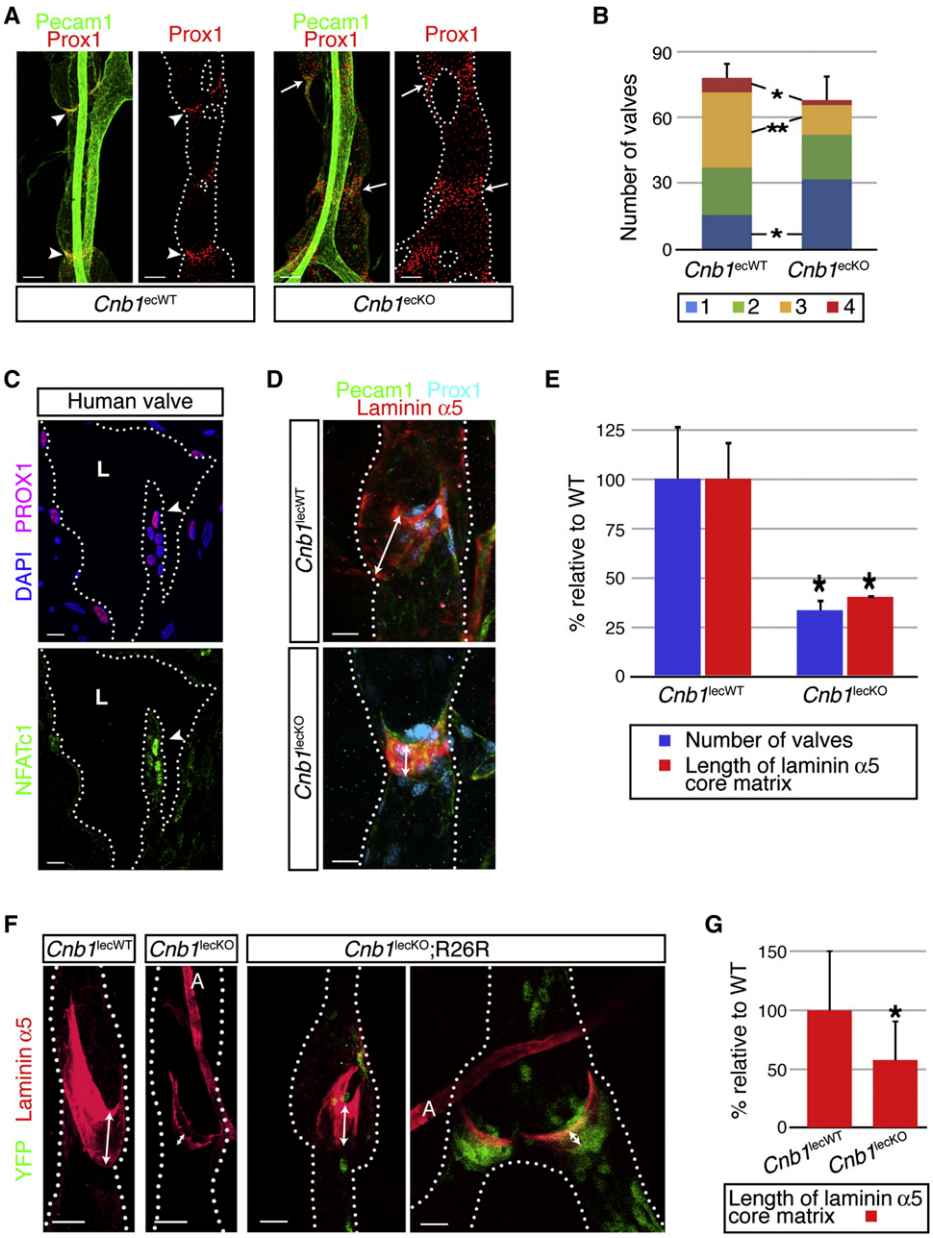

Figure 3. Cell-Autonomous Calcineurin Signaling Controls Lymphatic-Valve Morphogenesis and Maintenance

(A) Lymphatic valve formation is impaired in *Cnb1*^{ecKO} mice. E18.5 mesenteric vessels were stained for Prox1 (red) and Pecam1 (green). ecKO, endothelial cell knock-out; ecWT, wild-type. Arrowheads indicate mature lymphatic valves; arrows point to failure of valve condensation in *Cnb1*^{ecKO} mice. Bar, 100 μm.

(B) Quantification of lymphatic valves and their maturation stage at E18.5. Stages of valve development are as in Figure 1B. *$p < 0.05$, **$p < 0.001$, $n = 10$ embryos per genotype. ecKO, endothelial cell knock-out; ecWT, wild-type.

(C) Activated NFATc1 in adult human lymphatic valve. Cells were stained for PROX1 (pink), NFATc1 (green), and DNA (blue). Arrowheads indicate the lymphatic valve leaflet. L, lumen. Bar, 10 μm.

(D) Postnatal loss of *Cnb1* leads to valve degeneration. P7 mesenteric vessels from *Cnb1*^{lecKO} or the control mice stained for Pecam1 (green), Prox1 (blue), and laminin α5 (red). The double arrow indicates the valve laminin α5 ECM core. lecKO, lymphatic endothelial cell knock-out; lecWT, wild-type. Bar, 20 μm.

(E) Quantification of valve number (blue bars) and ECM core length (red bars) in mesenteric vessels of P7 *Cnb1*^{lecKO} or the control mice. *$p < 0.05$, $n = 6$ pups per genotype. lecKO, lymphatic endothelial cell knock-out; lecWT, wild-type.

(F) Adult lymphatic valves require continuous calcineurin signaling. Ear lymphatic vessels of the control *Cnb1*^{lecWT}, *Cnb1*^{lecKO} and *Cnb1*$^{f/f}$;ROSA26R-YFP;*Prox1*-CreERT2 mice were stained for YFP (green) and laminin α5 (red). YFP indicates sites of Cre-recombination. Note the normal development of YFP-negative lymphatic valve and shortened laminin α5 ECM core in YFP-expressing valves. The double arrow indicates the laminin α5 ECM core of the valve leaflet. A, arteriole. lecKO, lymphatic endothelial cell knock-out; lecWT, wild-type. Bar, 20 μm.

(G) Quantification of laminin α5 ECM core length in adult *Cnb1*^{lecKO} or control mice. *$p < 0.05$, $n = 10$ valves per mouse. lecKO, lymphatic endothelial cell knock-out; lecWT, wild-type.

See also Figure S3. All values are means ± SD.

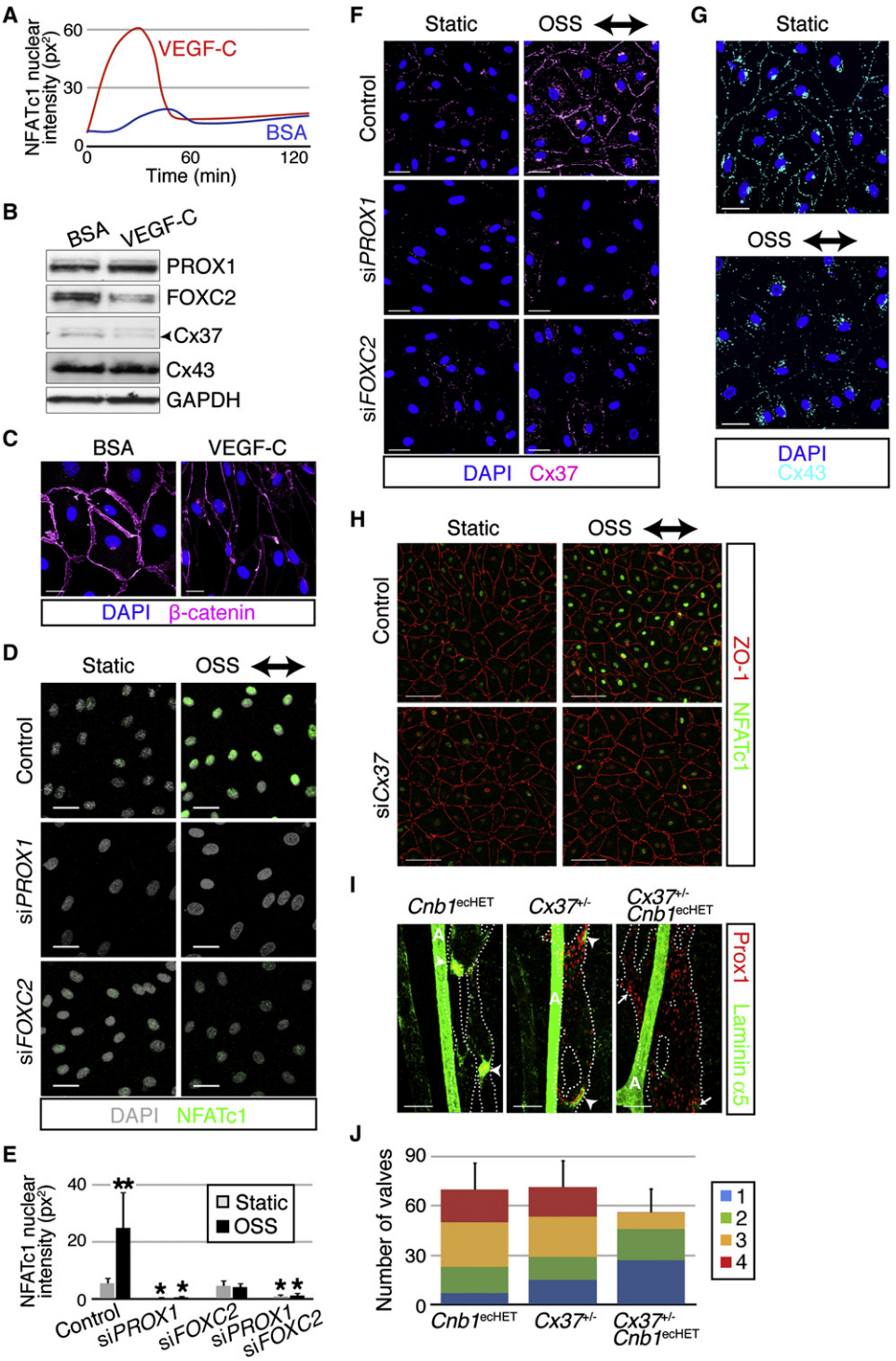

Figure 4. PROX1, FOXC2, and Shear Stress, but not VEGF-C, Coordinately Control Expression of Cx37 and Sustained Activation of Calcineurin/NFATc1 in Lymphatic Endothelial Cells

(A) Transient activation of calcineurin/NFATc1 in LECs in response to VEGF-C and quantification of nuclear NFATc1 in LECs treated with VEGF-C (red line) or BSA (blue line).

(B) VEGF-C suppresses FOXC2 and Cx37 expression at 24 hr. Western blot for the indicated proteins.

(C) VEGF-C induces elongation of LECs. β-catenin (pink) and DNA (blue) in LECs treated with VEGF-C or BSA for 24 hr.

(D) PROX1- and FOXC2-dependent NFATc1 activation by oscillatory shear stress. LECs transfected with AllStars control, *PROX1*, or *FOXC2* siRNAs, were subjected to OSS or left under static conditions for 48 hr. NFATc1 (green), DNA (gray). The threshold of NFATc1 detection was set up to detect only nuclear NFATc1. Bar, 50 μm.

calcineurin/NFAT signaling. Furthermore, heterozygous loss of *Cx37* and calcineurin in endothelial cells synergistically impaired the development of lymphatic valves. The resulting phenotype was reminiscent of homozygous loss of *Cnb1*, in which LVCs fail to condense (Figures 4I and 4J). Taken together, these data suggest that Cx37 acts upstream of calcineurin/NFAT and lend support to a model in which Cx37 and calcineurin belong to a mechanotransduction cascade downstream of PROX1 and FOXC2.

Oscillatory Fluid Shear Stress Induces Lymphatic Valve-Forming Cell Characteristics in Cultured Lymphatic Endothelial Cells

To study whether flow regulates other LVC characteristics, we analyzed cell shape and actin cytoskeleton organization in LECs subjected to OSS or laminar shear stress (LSS), as a control. As described previously, under static conditions, LECs had variable shape and size and cortical actin cytoskeleton (Petrova et al., 2002; Figure 5A). OSS induced a cuboidal cell shape (length/width ratio close to 1) and increased the amount of short perinuclear F-actin stress fibers (Figures 5A and 5B), a phenotype similar to the one observed in LVCs in vivo (Figure S1C). Exposure to LSS resulted in moderate LEC elongation and formation of stress fibers, aligned in the flow direction (Figures 5A–5C). Thus, LECs under static, OSS, and LSS conditions are characterized by distinct cytoskeletal organization and morphology. Exposure to OSS results in the formation of cuboidal cells, reminiscent of LVCs in vivo, whereas cells under LSS elongate and align in flow, reproducing lymphangion cell morphology.

We next investigated how OSS and LSS affect the expression of blood endothelial shear-stress-responsive genes KLF2 and eNOS (Boon and Horrevoets, 2009). As reported previously for blood endothelial cells, only LSS induced KLF2 mRNA (Figure 5D). Both OSS and LSS induced eNOS mRNA and protein in comparison to static conditions (Figures 5D and 5E), suggesting that eNOS is an indicator of flow onset in lymphatic vessels in vivo. We also studied whether the two types of flow regulate the expression of LYVE-1 and NRP2, which are selectively downregulated in LVCs in vivo (Figures 1D and 1G). OSS and, to a lesser extent, LSS downregulated LYVE-1, while OSS specifically decreased NRP2 mRNA and protein (Figures 5F and 5G).

We next studied whether flow affects the expression of PROX1 and FOXC2. OSS, but not LSS, upregulated FOXC2, whereas PROX1 was not affected (Figure 5H). While induction of *Cx37* required both PROX1 and OSS (Figure 4F), the expression of PROX1 target gene *VEGFR*-3 was not significantly modified under these conditions (Yoshimatsu et al., 2011; Figure 5I). Thus, PROX1 appears to have both constitutive and shear-stress-inducible transcriptional activities. Collectively, these results suggest that in vitro OSS reproduces many, albeit not all, features of LVCs, such as downregulation of LYVE-1, NRP2, and Cx43, a switch to cuboidal cell shape, enhanced expression of FOXC2 and Cx37, and activation of calcineurin/NFAT.

PROX1 and FOXC2 Control LEC Cytoskeletal Reorganization and Cell Alignment in Response to Flow

We investigated next whether PROX1 and FOXC2 control cytoskeletal responses of LECs to shear stress. PROX1-depleted cells had highly variable shape and size, and they were unable to adopt the cuboidal shape under OSS (Figures 6A and 6B). *PROX1* knockdown promoted formation of long stress fibers, normally observed only in cells under LSS (Figure S5A). Even under static conditions, PROX1-depleted cells aligned in the long axis of the flow chamber (Figures 6A and 6C). Under LSS, loss of PROX1 dramatically enhanced cell elongation and alignment in the direction of flow, leading to the formation of very long and thin cells with a length/width ratio up to 35 (Figures 6A–6C). PROX1 depletion also decreased VE-cadherin at cell-cell contacts without affecting total VE-cadherin protein (Figures 6A, S4C, and S5B). In summary, these results show that loss of PROX1 abolishes the LEC response to OSS while it enhances cell elongation and alignment in response to LSS.

In contrast to PROX1 results, knockdown of *FOXC2* did not prevent cuboidal cell shape acquisition under OSS (Figures 6A and 6B). The most striking feature of FOXC2 depletion was the induction of circumferential thick actin fibers and star-like bundles (Figure S5A). Loss of FOXC2 also resulted in disorganization of adherens junctions under OSS conditions, suggesting impairment of junction integrity (Figure S5B). Cells under LSS had enhanced cell elongation, although to a lesser degree compared to *PROX1* knockdown (Figures 6A–6C). Upon combined inactivation of *PROX1* and *FOXC2*, the behavior of cells under OSS was similar to that of *FOXC2* knockdown, whereas cells under LSS adopted the ultraelongated phenotype similar to *PROX1* depletion (Figures 6A–6C). Altogether, these results indicate that FOXC2 and PROX1 have similar effects on calcineurin activation and Cx37 expression in response to shear stress, but they play distinct roles in the organization of actin cytoskeleton and cell-cell junctions in LECs subjected to flow.

Differential Levels of PROX1 and FOXC2 Induce Cell Segregation

Isolated LVCs (Figures 1C and S1B) are rarely observed after the onset of valve formation. Thus, we asked whether differential levels of Prox1 and Foxc2 might be responsible for LVC clustering and formation of lymphatic-valve territory. To test this hypothesis, we mixed PROX1^{high}/FOXC2^{high} (as a model of LVCs, transfected with control siRNA) and PROX1^{low}/FOXC2^{low} LECs (as a model of lymphangion cells, transfected with *PROX1* and *FOXC2* siRNAs) and evaluated cell segregation. To

(E) Quantification of nuclear NFATc1. *p < 0.001 versus control siRNA; **p < 0.001 versus static conditions.
(F) PROX1- and FOXC2-dependent induction of *Cx37* by oscillatory shear stress. Cells were stained for Cx37 (pink) and DNA (blue). Bar, 30 μm.
(G) Oscillatory shear stress decreases Cx43, as shown by staining for Cx43 (cyan) and DNA (blue). Bar, 30 μm.
(H) Cx37 depletion prevents uniform calcineurin/NFATc1 activation in response to shear stress. Staining for NFATc1 (green) and ZO-1 (red). Bar, 100 μm.
(I) Genetic interaction between Cx37 and calcineurin signaling in E18.5 mesenteric vessels stained for Prox1 (red) and laminin α5 (green). The arrowheads indicate valve sites at stages 3 and 4, and the arrow indicates the valve site at stage 1. A, artery. Bar, 100 μm.
(J) Number of mesenteric lymphatic valves at different stages in E18.5 *Cnb1*^{ecHET}, *Cx37*$^{+/-}$ (n = 4 embryos per genotype) and double *Cnb1*^{ecHET}; *Cx37*$^{+/-}$ (n = 2) embryos. Stages of valve development are as in Figure 1B.
See also Figure S4. All values are means ± SD.

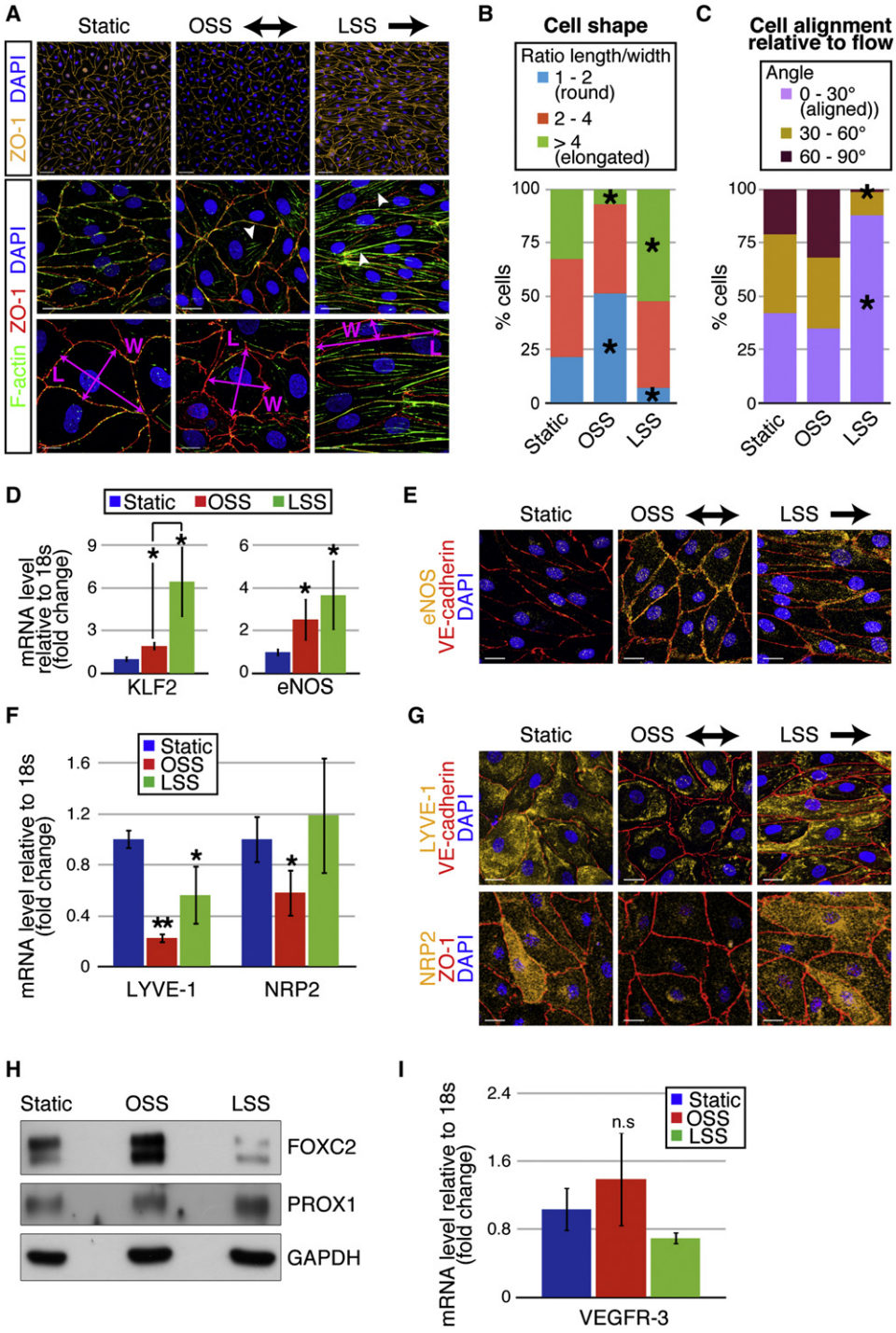

Figure 5. In Vitro Oscillatory Shear Stress Reproduces Features of Lymphatic-Valve-Forming Cells

(A) Cell shape and actin cytoskeleton organization in LECs under static, oscillatory (OSS), or laminar (LSS) conditions. Top: cells are cuboidal in OSS and are elongated and aligned in the direction of flow in LSS. Cells were stained for ZO-1 (yellow) and DNA (blue). Bar, 50 μm. Middle and bottom panels: cortical F-actin in cells under static conditions, OSS induces short perinuclear stress fibers and LSS induces long stress fibers aligned in the flow direction. Cells were stained for ZO-1 (red), F-actin (green), and DNA (blue). Arrowheads indicate actin stress fibers. Bottom: cell length (L) and width (W) were used for quantification of cell-shape changes and alignment relative to flow. Bar, 20 μm.

(B) Quantification of cell shape in static, OSS, or LSS conditions. The cell is round when L/W = 1. *$p < 0.001$.

(C) Quantification of cell alignment under static, OSS, or LSS conditions. Cell is aligned with the flow when the angle between its length and the flow direction is 0°. In the static condition, the long axis of the flow chamber was used for the measurements. *$p < 0.001$.

(D) Regulation of KLF2 and eNOS mRNA by shear stress. RT-qPCR was used for the indicated transcripts. *$p < 0.01$.

distinguish between cell populations, PROX1^{high}/FOXC2^{high} LVC-like cells were labeled with a fluorescent membrane-permeant dye (Figure S5C). As a control, we used a mix of labeled and unlabeled LECs transfected with the control siRNA (homogeneous population). When comparing these two conditions, we found that the heterogeneous population had a reduced number of isolated single-labeled cells (15% versus 21% in the homogeneous population) and an increased number of cells assembled into large clusters (38% versus 21% in the homogeneous population) (Figures 6D and 6E), leading to the establishment of valve-like territories in vitro. There was no difference between static and OSS conditions (Figures 6D and 6E), indicating that cell segregation depends on PROX1 and FOXC2, but not mechanical stimulation. Importantly, only PROX1^{high}/FOXC2^{high} LVC-like, and not PROX1^{low}/FOXC2^{low} cells, accumulated nuclear NFATc1 under OSS (Figure 6D). Thus, differential levels of PROX1 and FOXC2 are sufficient to induce cell segregation, whereas shear stress activates distinct signaling in the two cell types, providing a mechanism for further amplification of initial differences between the two adjacent cell populations.

To test what cell-surface molecules mediate cell segregation, we studied the role of VE-cadherin, upregulated in LVCs (Figure 1C), or Nrp2, downregulated in LVCs (Figure 1G). VE-cadherin^{high} LVC-like cells segregated from VE-cadherin^{low} cells (64% labeled cells in large clusters versus 15% in a homogeneous population), whereas loss of NRP2 had no effect (Figures 6F, 6G, S5F, and S5G). These results thus suggest that the high levels of VE-cadherin observed in LVCs contribute to the establishment of the valve territory.

In Vivo Analysis of Lymphatic Flow

Data on lymphatic flow during mouse embryonic development are scarce. LECs arise in embryonic veins from E9.5 and begin sprouting around E10.5. However, *Vegfc*$^{-/-}$ and *Prox1*$^{-/-}$ embryos, which lack lymphatic vessels, die by E15.5 (Karkkainen et al., 2004; Wigle and Oliver, 1999), suggesting that lymph drainage becomes critical from this point onward. eNOS was induced in LECs in vitro by shear stress (Figure 5E), suggesting that eNOS can be used as a marker of increased flow in vivo. eNOS was low in immature mesenteric lymphatic vessels at E15.0 (Figure 7A). In contrast, increased levels of eNOS and podocalyxin, a sialomucin of the endothelial glycocalyx necessary for shear-stress-induced NO production (Tarbell and Ebong, 2008), were observed at later stages in E15.5 collecting lymphatic vessels before the appearance of Prox1^{high} LVCs (Figures 7A and 7B), suggesting that flow increase precedes lymphatic valve formation.

We next studied embryonic lymphatic flow using fluorescent lymphangiography. Lymph flow was present in E16.0 embryos, but it was reversing in many areas, especially at vessel bifurcations, in line with the absence of formed lymphatic valves at this stage (Figure 7C and Movie S1). In contrast, flow was mostly directional at E18.5, when lymphatic valves are formed (Figure 7D and Movie S1). To confirm the identity of the dye-filled vessels, we injected *Prox1*-mOrange2 embryos in which lymphatic vessels are genetically marked by a fluorescent protein (Figure S6). At E14.5 flow was almost absent despite the presence of lymphatic vessels (Figure S6C; data not shown), but starting from E15.5, lymphatic-vessel filling and drainage were observed (Figure 7E).

We next visualized adult lymphatic-valve dynamics (Figure 7F and Movie S2) and the unidirectional pulsatile lymphatic flow using a skinfold chamber model (Movie S3). In agreement with the flow pattern reported in venous valves (Chiu and Chien, 2011), we observed nondirectional movement of autofluorescent particulate material in the lymphatic-valve sinuses (Movie S3), suggesting flow recirculation in this area. Based on in vitro and in vivo data, we propose that flow recirculation in mature lymphatic valve sinuses maintains high levels of Foxc2, Cx37, activated calcineurin/NFATc1, and eNOS, while it represses Nrp2 (Figure 7G).

Studies of mechanotransduction in developing blood vessels rely on the possibility of modifying blood-flow velocity by altering heart-pumping activity (Adamo et al., 2009; May et al., 2004; Vermot et al., 2009). Lymphatic flow is not driven by a central pump, but rather by the local compression of surrounding tissues; thus, the methods developed to study developmental hemodynamics cannot be applied. Therefore, we studied lymphatic vessels cultured ex vivo, in which compression of surrounding tissues is abrogated. Ex vivo culture led to disassembly of lymphatic-valve territories and loss of patterned expression of Prox1 and Foxc2 (Figure 7H). Although alternative explanations are possible, these data suggest that the development of lymphatic valves requires mechanical stimulation.

DISCUSSION

This study defines the molecular mechanisms of a fascinating vascular morphogenetic event, the formation of lymphatic valves. We show that lymphatic-valve-forming endothelial cells are characterized by distinct morphological and molecular properties (Figure 1K). Furthermore, we establish a hierarchy of molecular events during early stages of lymphatic valve development (Figure S7). Prox1 and Foxc2 act as upstream regulators of *Cx37* expression and calcineurin/NFAT activation, which in turn contribute to different steps of lymphatic valve formation: assembly of lymphatic-valve-forming cells into a ring-like structure, valve-territory delimitation, and postnatal valve maintenance (Figure S7). Importantly, flow coordinately induces Cx37 expression and calcineurin activation in vitro, and this response requires both Prox1 and Foxc2. We thus propose that the cooperation between lymphatic endothelial transcription factors Foxc2 and Prox1 and mechanical forces is essential for lymphatic-valve morphogenesis (Figure S7).

(E) Both LSS and OSS induce eNOS protein in comparison to static conditions. Cells were stained for eNOS (orange), VE-cadherin (red), and DNA (blue).
(F) OSS decreases LYVE-1 and NRP2 mRNA. RT-qPCR was used for the indicated transcripts. *$p < 0.01$, **$p < 0.001$.
(G) OSS downregulates LYVE-1 and NRP2 proteins. Cells were stained for LYVE-1 or NRP2 (orange), VE-cadherin, or ZO-1 (red) and DNA (blue). Bar, 20 μm.
(H) OSS increases FOXC2, as shown by western blot for the indicated proteins.
(I) VEGFR-3 is not significantly regulated by low shear stress, as shown by RT-qPCR. n.s., not significant; LSS, laminar shear stress; OSS, oscillatory shear stress. All values are means ± SD.

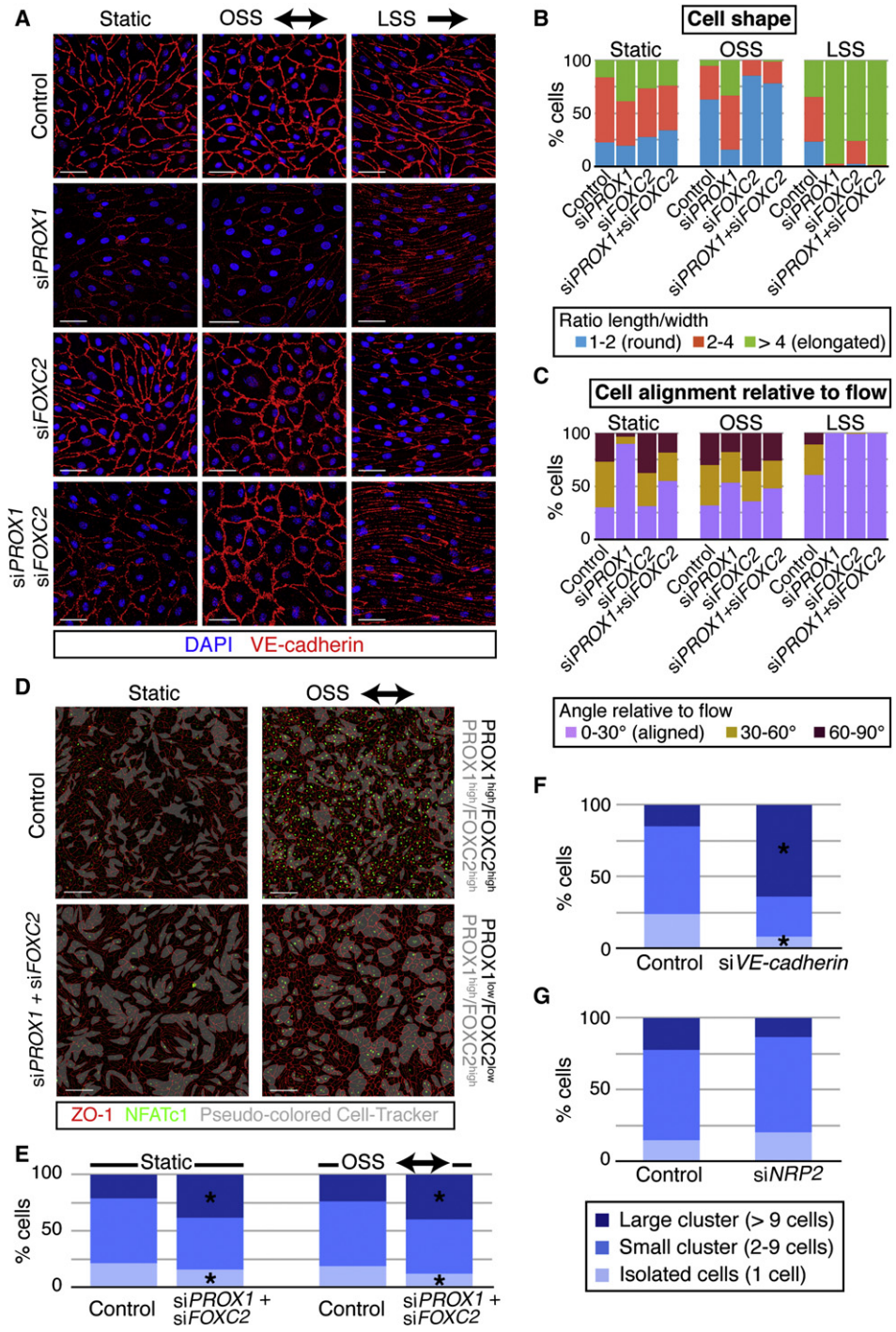

Figure 6. PROX1 and FOXC2 Control Mechanotransduction and Clustering of Lymphatic Endothelial Cells

(A) Effects of shear stress on LEC shape in the presence and in the absence of PROX1 and/or FOXC2. Cells were stained for VE-cadherin (red) and DNA (blue). Bar, 50 μm.

(B) Quantification of cell-shape changes.

(C) Quantification of changes in cell alignment relative to flow direction.

(D) PROX1^{high}/FOXC2^{high} and PROX1^{low}/FOXC2^{low} cells segregate in two different populations. CellTracker labeled PROX1^{high}/FOXC2^{high} were mixed with unlabeled PROX1^{low}/FOXC2^{low} or PROX1^{high}/FOXC2^{high}, as a control, and subjected to OSS or left under static conditions. Cells were stained for ZO-1 (red), CellTracker (gray), and NFATc1 (green). For visualization, CellTracker-labeled cells are pseudocolored in gray. Figure S5C shows an example of the original image.

(E) Quantification of cell cluster formation. *p < 0.001.

(F and G) Differential levels of VE-cadherin but not NRP2 contribute to LEC segregation. *p < 0.001. LSS, laminar shear stress; OSS, oscillatory shear stress. See also Figure S5.

Lymphatic Endothelial Transcription Factors as Regulators of Mechanotransduction

Flow plays an important role in the morphogenesis of blood vessels. Here we report that PROX1 and FOXC2 regulate multiple aspects of lymphatic endothelial cell response to fluid shear stress in vitro, such as cytoskeletal rearrangement, cell shape remodeling, and cell alignment. A close link between the transcription factors PROX1 and FOXC2 and mechanosensory signal transduction in LECs also demonstrates that endothelial cell identity shapes cellular responses to mechanical stimulation. This idea is also in line with differential responses of lymphatic and blood vascular endothelial cells to interstitial flow (Ng et al., 2004). Further analysis of PROX1- and FOXC2-dependent mechanosensitive genes should provide detailed information on the molecular mechanisms involved.

A number of lymphatic endothelial cell responses to shear stress, such as Cx37 expression and calcineurin/NFAT activation, are regulated by both PROX1 and FOXC2, suggesting cooperation between these two transcription factors. In line with these observations, we observed a 15%–20% overlap in gene-expression profiles of LECs following the knockdown of *PROX1* or *FOXC2* under static conditions (unpublished data). Direct comparison of gene-expression profiles and FOXC2/PROX1 binding sites using ChIP/RNA-seq from LECs subjected to flow should reveal whether this transcriptional overlap is due to co-occupancy of common enhancers or interaction of signaling pathways on a higher level.

In vitro comparison of oscillatory versus laminar flow revealed that OSS induces many characteristics of lymphatic valve-forming cells, while LSS confers a lymphangion-like phenotype. Taken together with the in vivo analysis of flow during development, these results support a model in which reversing flow contributes to the formation of lymphatic valves (Figure S7). This model also explains why lymphatic valves are frequently formed at vessel bifurcations (Figure S1G), as these regions are more likely to have flow recirculation (Chiu and Chien, 2011; Hahn and Schwartz, 2009). Developing lymphatic vessels in vivo are subjected to highly variable mechanical forces, e.g., pulsatile and turbulent flow and mechanical stretching; therefore, future work should include more precise quantitative analysis of embryonic lymph flow in vivo and modeling of different conditions in vitro.

Molecular Control and Role of Connexin37 in Lymphatic-Valve Morphogenesis

Connexins play an important role for local and long-range instructive morphogenetic cues in development via the establishment of gap-junctional intercellular communication (Wei et al., 2004). Kanady et al. recently reported failure of lymphatic-valve formation and lymphatic drainage in $Cx37^{-/-}$ and $Cx37^{-/-}$; $Cx43^{+/-}$ mice (Kanady et al., 2011). Here we show that Cx37 controls the precise assembly of a circumferential lymphatic-valve territory, and we propose that Cx37 mediates cell-cell communication and collective long-range interactions in this process (Figure S7). Mechanistically, Cx37 acts downstream of Prox1, Foxc2, and shear stress, and it is required for a uniform calcineurin/NFAT activation in response to flow, thus providing a molecular framework for a stepwise model of lymphatic-valve morphogenesis. Potentially, Cx37 gap junctions may mediate transfer of IP_3, which triggers the release of intracellular Ca^{2+}, necessary for calcineurin/NFAT activation. This concept supports a putative gap-junction-mediated mechanism for establishment of a morphogenetic gradient proposed in 2002 (Crabtree and Olson, 2002). However, other mechanisms, such as connexin-mediated release of ATP (Wong et al., 2006) and increase of intracellular Ca^{2+} via activated purinergic receptors should also be considered.

Formation of lymphatic valves is perturbed in mice double heterozygous for *Cx37* and *Foxc2*, and FOXC2 interacts with a consensus site identified previously by ChIP-chip analysis (Norrmén et al., 2009) and located 44,286 bp upstream of *Cx37* transcription start site (Y. Agalarov, N. Houhou, and M. Delorenzi, unpublished data). These results further strengthen the notion that *Cx37* is a direct target of FOXC2 and suggest that decreased Cx37 is one of the reasons for incompetent valves observed in patients with *FOXC2* mutations (Brice et al., 2002; Mellor et al., 2007).

Calcineurin/NFAT Pathway in Vascular Morphogenesis

In vitro studies postulated that calcineurin/NFAT mediates most VEGF/VEGFR-2-induced responses of endothelial cells, including cell proliferation, migration, and tube formation (Hernández et al., 2001; Johnson et al., 2003; Schweighofer et al., 2009; Zaichuk et al., 2004). Germline inactivation of calcineurin arrests vascular morphogenesis at the stage of primitive blood capillary plexus and prevents heart-valve development (Chang et al., 2004; Graef et al., 2001). Endothelium-specific loss of calcineurin leads to abnormal coronary-vessel development (Zeini et al., 2009), but the role of calcineurin in vascular development was not investigated in either model beyond E12.5. Our results show that, in contrast to the in vitro results, endothelial calcineurin/NFAT is dispensable for Vegf/Vegfr-2-driven angiogenesis after midgestation, while signaling in lymphatic vasculature is important for valve establishment and maintenance. These data further highlight the complexity and differential requirements for the calcineurin pathway during early and late developmental (lymph)angiogenesis.

How does shear stress activate calcineurin in lymphatic valve cells? In addition to its role in angiogenesis, VEGFR-2 is a component of the endothelial mechanosensory complex (Tzima et al., 2005), and it is highly expressed in lymphatic-valve-forming cells and mature lymphatic valves (Figure 1E and Saaristo et al., 2002). Therefore, it is one of the candidate cell surface sensors for activation of calcineurin/NFAT. Vegfr-2 forms heterodimers with Vegfr-3, and its coreceptor neuropilin-2. The latter, which is important for VEGF-C-induced sprouting of lymphatic capillaries (Xu et al., 2010), is selectively absent in developing and mature lymphatic valve cells (Figures 1D and S1D). It will be important to test in the future to what extent Vegfr-2/Vegfr-3 signal transduction cascades differ in sprouting capillaries versus lymphatic-valve-forming cells.

Our studies revealed a cell-autonomous requirement for calcineurin/NFAT activation in the maintenance of adult lymphatic valves. Lymphatic valves are the subject of intense shear stress (Dixon et al., 2006); thus, continuous calcineurin signaling may be necessary to ensure the survival of valve endothelial cells. PROX1 and FOXC2 are highly expressed in human and mouse venous-valve endothelial cells, which also show nuclear NFATc1 localization (Bazigou et al., 2011; our unpublished data), further

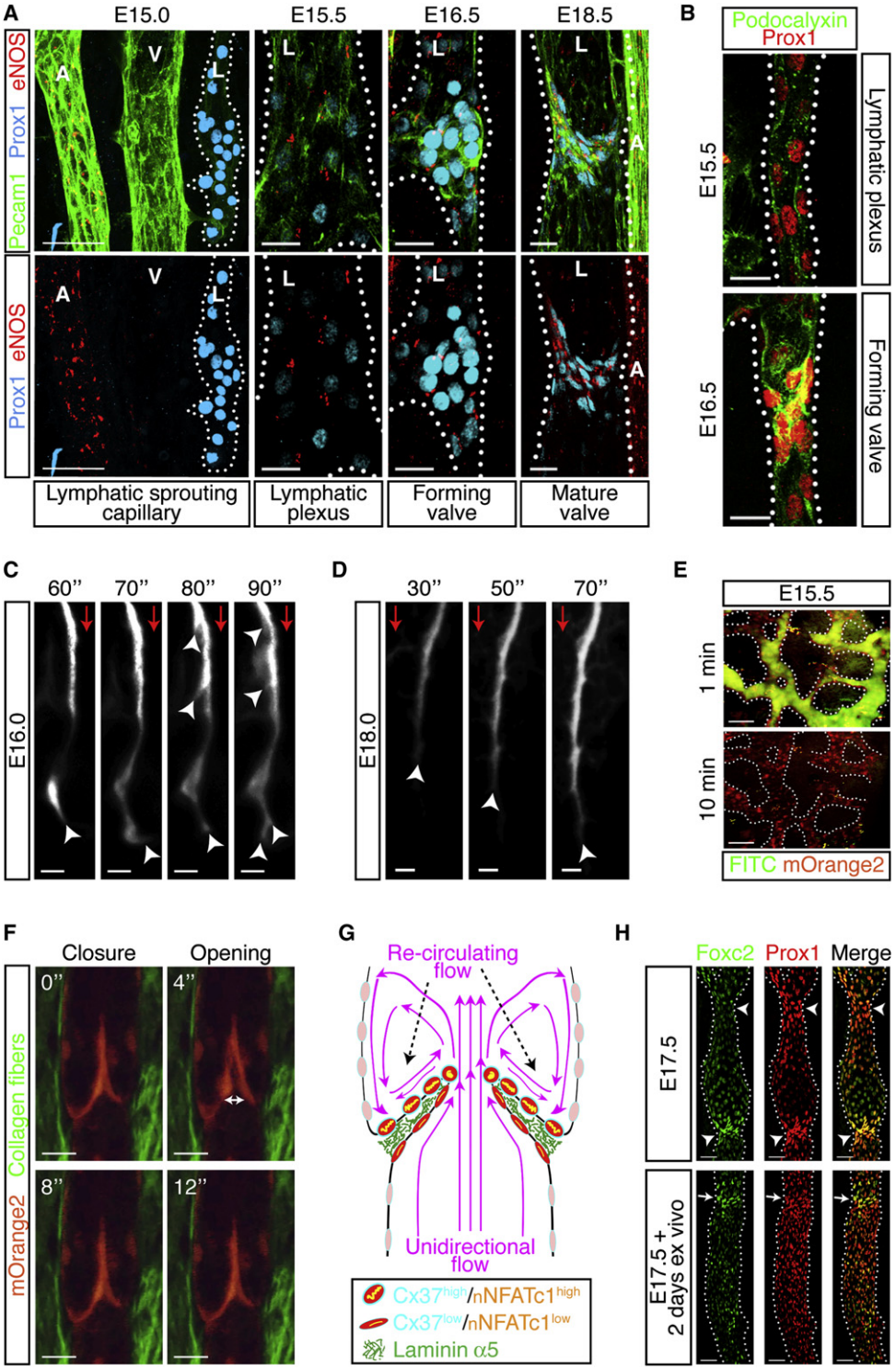

Figure 7. Analysis of Lymphatic Flow In Vivo

(A) Developing collecting vessels express eNOS before the onset of lymphatic valve formation at E15.5, and eNOS expression is higher in lymphatic-valve-forming cells and mature valves. Mesenteric vessels were stained for eNOS (red), Prox1 (blue), and Pecam1 (green). A, artery; V, vein; L, lymphatic vessel. Bar, 50 μm in left panel and 20 μm in the other panels.

(B) LVCs have higher levels of podocalyxin. E15.5 and E16.5 mesenteric vessels were stained for podocalyxin (green) and Prox1 (red). Bar, 20 μm.

(C and D) Examples of lymphatic flow in E16.0 or E18.0 embryos, injected with FITC-dextran (gray). Lymphatic flow is reversing in some areas at E16.0, but mostly directional at E18.0. Four time points for each stage of Movie S1 are shown. The red arrow shows the direction of lymph flow. The arrowheads indicate the end of the visible dye-filled vessel. Bar, 300 μm.

highlighting similarities between lymphatic and venous valves. These data also suggest that dysfunction of venous and/or lymphatic circulation may be one of the potential side effects of a long-term immunosuppressive therapy with cyclosporin A.

In conclusion, our study sheds light on early steps of lymphatic valve morphogenesis and suggests an important contribution of mechanical forces to this remodeling process, which act in concert with the transcription factors Prox1 and Foxc2. We introduce Cx37 and calcineurin/NFATc1 signaling as mechanoresponsive pathways in the lymphatic endothelium and downstream effectors of Prox1 and Foxc2, where they act at different stages of lymphatic-valve formation. Our results show how local increases in the level or activation status of transcription factors, together with mechanical stimulation, can be translated into a discrete cell signaling pattern and morphogenetic event. They also suggest that endothelial cell identity controls mechanosensory signal transduction and vascular remodeling.

EXPERIMENTAL PROCEDURES

Animal Models

Animal experiments were approved by the Animal Ethics Committee of Vaud, Switzerland, and by the Animal Experimentation Committee of the county of Münster, Germany. We used *Cnb1*$^{f/f}$, *Cx37*$^{-/-}$, *Cdh5(PAC)-CreERT2, PDGFb-iCreERT2, Prox1*-CreERT2, ROSA26R-YFP, and *Foxc2*$^{-/-}$ mice (Bazigou et al., 2011; Claxton et al., 2008; Iida et al., 1997; Simon et al., 1997; Wang et al., 2010; Zeng et al., 2001). *Prox1*-mOrange2 mice (Hagerling et al., 2011), tamoxifen treatment, ex vivo culture, antibodies, and staining procedures are described in the Supplemental Experimental Procedures.

In Vivo Analyses

For microlymphangiography, we injected anesthetized adult mice with 5 μl of 8 mg/ml FITC-dextran (2,000 kDa) or 10 mg/ml Evans Blue in PBS. We injected E16.5 and E18.5 embryos with 0.5 μl of FITC-dextran in the upper hindlimb, and E14.5 and E15.5 embryos in the buccal region. Embryo viability was monitored by heart beat and blood flow. Mice were observed under a Leica M205FA stereomicroscope equipped with DFC300FXR2 camera (Leica) and the software LAS AF6000, or under a customized two-photon microscope (TrimScope, LaVision BioTec) and Olympus 20× NA = 0.95 water immersion objective. Imaging parameters are described in the Supplemental Experimental Procedures. In adult mice lymph vessels were imaged using a dorsal skinfold chamber (Lehr et al., 1993). All images of whole-mount staining are shown in the same orientation, i.e., with the direction of flow from bottom to top.

Cell Culture, Transfection, RNA Isolation, qPCR, and Western Blot Analyses

Human LECs and mouse endothelial cells, VEGF-C treatment, siRNA transfection, RNA isolation, reverse transcription, amplification, qPCR, and western blotting analyses are described in the Supplemental Experimental Procedures. RT-qPCR and/or western blot analysis confirmed target mRNA or protein depletion (Figures S4C, S4F, S4G, S5D, and S5E).

In Vitro Flow Analysis

Confluent LECs on fibronectin-coated slides (μ-Slide I$^{0.8}$ Luer; ibidi) were subjected to laminar (4 dyn/cm^2) or oscillatory (4 dyn/cm^2, ¼ Hz) flow in a parallel-plate flow-chamber system (ibidi Pump System, ibidi) or kept under static conditions for 48 hr. Shear-stress parameters were chosen based on the measurements reported by Zawieja, (2009). For cell segregation studies, LECs were transfected with *PROX1*, *FOXC2, VE-cadherin*, *NRP2*, or control siRNAs. Labeled PROX1^{high}/FOXC2^{high} (20% or 30%, transfection with AllStars siRNA, labeled with CellTracker Orange CMRA dye, Molecular Probes, Invitrogen) and unlabeled PROX1^{low}/FOXC2^{low} (80% or 70%, transfection with *PROX1* and *FOXC2* siRNAs) cells were mixed, plated at confluence, and subjected to flow or left under static conditions. Similar experiments were carried out using mixtures of VE-cadherin$^{high/low}$ or NRP2$^{high/low}$ cells.

Quantification and Statistical Analysis

The number of valves at each developmental stage (Figure 1B) was quantified using four mesenteric vessels in 3–10 mice/genotype. For *Cnb1; Cx37; Cdh5(PAC)-CreERT2* crosses two double heterozygous embryos from different litters and eight littermate controls were analyzed. Laminin α5 leaflet ECM core was measured using ImageJ software on three mesenteric vessels of neonates or 10 randomly chosen ear valves of adult mice. For flow experiment quantification, the ratio of cell length to width, axis of cell elongation, and its angle to flow direction defined as in Figure 5A were calculated using ImageJ and 100–200 cells per experiment. We quantified nuclear NFATc1 using ImageJ *Mean Gray Value* function. Size of cell cluster, defined as a group of labeled cells in contact with each other, was measured by counting the number of cells in the cluster.

A two-tailed, unpaired Student's t test was done to determine statistical significance by calculating the probability of difference between two means. The differences were considered statistically significant at $p < 0.05$. Data are shown as mean ± SD.

SUPPLEMENTAL INFORMATION

Supplemental Information includes seven figures, Supplemental Experimental Procedures, and three movies and can be found with this article online at doi:10.1016/j.devcel.2011.12.020.

ACKNOWLEDGMENTS

We thank M. Fruttiger for *Pdgfß*-iCreERT2 mice, D.A. Goodenough and A. Simon for *Cx37*$^{-/-}$ mice, L. Sorokin for laminin α5 antibodies, M. Jeltsch and K. Alitalo for VEGF-C, N. Harvey for the LEC isolation protocol, M. Delorenzi and N. Houhou for bioinformatics analysis, and C. Cornu and D. Bachmann for mouse genotyping and help with immunohistochemistry. Animal, Cellular Imaging, Genomic Technologies, and Mouse Pathology Facilities of the University of Lausanne are gratefully acknowledged. This work was supported by Swiss National Science Foundation (PPP0033-114898 to T.V.P. and 310030_127551 to B.R.K.), Leenaards Foundation, Lymphatic Research Foundation (to H.M.-E.H.), Telethon and Emma Muschamp Foundations, and the German Research Foundation (SFB629 and SFB656 to F.K.)

(E) Drainage of FITC-dextran in E15.5 *Prox1*-mOrange2 embryos. Lymphatic vessels (red) are filled with FITC-dextran (green) 1 min after the injection, and the dye is drained by 10 min postinjection. Bar, 100 μm.
(F) Visualization of lymphatic-valve dynamics in live *Prox1*-mOrange2 adult mice in a skinfold chamber. Four time points of Movie S2 are shown, highlighting the lymphatic vessels (orange) and collagen fibers (green). The double arrow shows the valve opening. Bar, 20 μm.
(G) LECs in the valve sinuses subjected to flow recirculation express higher levels of Foxc2, Cx37 (blue), and nuclear NFATc1 (yellow), while cells on the luminal side are subjected to laminar flow and have lower levels of these proteins.
(H) Loss of Prox1 and Foxc2 patterning in collecting lymphatic vessels cultured ex vivo. E17.5 mesenteric vessels were stained immediately after dissection or after 2 days of culture. Arrowheads show the forming lymphatic valve, and the arrows point to the disorganized lymphatic valve site. Bar, 100 μm.
See also Figure S6 and Movies S1, S2, and S3.

Received: March 31, 2011
Revised: September 29, 2011
Accepted: December 22, 2011
Published online: February 2, 2012

REFERENCES

Adamo, L., Naveiras, O., Wenzel, P.L., McKinney-Freeman, S., Mack, P.J., Gracia-Sancho, J., Suchy-Dicey, A., Yoshimoto, M., Lensch, M.W., Yoder, M.C., et al. (2009). Biomechanical forces promote embryonic haematopoiesis. Nature *459*, 1131–1135.

Bazigou, E., Xie, S., Chen, C., Weston, A., Miura, N., Sorokin, L., Adams, R., Muro, A.F., Sheppard, D., and Makinen, T. (2009). Integrin-alpha9 is required for fibronectin matrix assembly during lymphatic valve morphogenesis. Dev. Cell *17*, 175–186.

Bazigou, E., Lyons, O.T., Smith, A., Venn, G.E., Cope, C., Brown, N.A., and Makinen, T. (2011). Genes regulating lymphangiogenesis control venous valve formation and maintenance in mice. J. Clin. Invest. *121*, 2984–2992.

Beis, D., Bartman, T., Jin, S.W., Scott, I.C., D'Amico, L.A., Ober, E.A., Verkade, H., Frantsve, J., Field, H.A., Wehman, A., et al. (2005). Genetic and cellular analyses of zebrafish atrioventricular cushion and valve development. Development *132*, 4193–4204.

Boon, R.A., and Horrevoets, A.J. (2009). Key transcriptional regulators of the vasoprotective effects of shear stress. Hamostaseologie *29*, 39–40, 41–43.

Brice, G., Mansour, S., Bell, R., Collin, J.R., Child, A.H., Brady, A.F., Sarfarazi, M., Burnand, K.G., Jeffery, S., Mortimer, P., and Murday, V.A. (2002). Analysis of the phenotypic abnormalities in lymphoedema-distichiasis syndrome in 74 patients with FOXC2 mutations or linkage to 16q24. J. Med. Genet. *39*, 478–483.

Chang, C.P., Neilson, J.R., Bayle, J.H., Gestwicki, J.E., Kuo, A., Stankunas, K., Graef, I.A., and Crabtree, G.R. (2004). A field of myocardial-endocardial NFAT signaling underlies heart valve morphogenesis. Cell *118*, 649–663.

Chiu, J.J., and Chien, S. (2011). Effects of disturbed flow on vascular endothelium: pathophysiological basis and clinical perspectives. Physiol. Rev. *91*, 327–387.

Claxton, S., Kostourou, V., Jadeja, S., Chambon, P., Hodivala-Dilke, K., and Fruttiger, M. (2008). Efficient, inducible Cre-recombinase activation in vascular endothelium. Genesis *46*, 74–80.

Crabtree, G.R., and Olson, E.N. (2002). NFAT signaling: choreographing the social lives of cells. Cell Suppl. *109*, S67–S79.

Dixon, J.B., Greiner, S.T., Gashev, A.A., Cote, G.L., Moore, J.E., and Zawieja, D.C. (2006). Lymph flow, shear stress, and lymphocyte velocity in rat mesenteric prenodal lymphatics. Microcirculation *13*, 597–610.

Graef, I.A., Chen, F., Chen, L., Kuo, A., and Crabtree, G.R. (2001). Signals transduced by $Ca^{(2+)}$/calcineurin and NFATc3/c4 pattern the developing vasculature. Cell *105*, 863–875.

Hagerling, R., Pollmann, C., Kremer, L., Andresen, V., and Kiefer, F. (2011). Intravital two-photon microscopy of lymphatic vessel development and function using a transgenic Prox1 promoter-directed mOrange2 reporter mouse. Biochem. Soc. Trans. *39*, 1674–1681.

Hahn, C., and Schwartz, M.A. (2009). Mechanotransduction in vascular physiology and atherogenesis. Nat. Rev. Mol. Cell Biol. *10*, 53–62.

Hernández, G.L., Volpert, O.V., Iñiguez, M.A., Lorenzo, E., Martínez-Martínez, S., Grau, R., Fresno, M., and Redondo, J.M. (2001). Selective inhibition of vascular endothelial growth factor-mediated angiogenesis by cyclosporin A: roles of the nuclear factor of activated T cells and cyclooxygenase 2. J. Exp. Med. *193*, 607–620.

Iida, K., Koseki, H., Kakinuma, H., Kato, N., Mizutani-Koseki, Y., Ohuchi, H., Yoshioka, H., Noji, S., Kawamura, K., Kataoka, Y., et al. (1997). Essential roles of the winged helix transcription factor MFH-1 in aortic arch patterning and skeletogenesis. Development *124*, 4627–4638.

Johnson, E.N., Lee, Y.M., Sander, T.L., Rabkin, E., Schoen, F.J., Kaushal, S., and Bischoff, J. (2003). NFATc1 mediates vascular endothelial growth factor-induced proliferation of human pulmonary valve endothelial cells. J. Biol. Chem. *278*, 1686–1692.

Kampmeier, O.F. (1928). The genetic history of the valves in the lymphatic system of man. Am. J. Anat. *40*, 413–457.

Kampmeier, O.F., and Brich, L.F. (1927). The origin and development of the venous valves, with particular reference to the saphenous district. Am. J. Anat. *38*, 451–499.

Kanady, J.D., Dellinger, M.T., Munger, S.J., Witte, M.H., and Simon, A.M. (2011). Connexin37 and Connexin43 deficiencies in mice disrupt lymphatic valve development and result in lymphatic disorders including lymphedema and chylothorax. Dev. Biol. *354*, 253–266.

Karkkainen, M.J., Haiko, P., Sainio, K., Partanen, J., Taipale, J., Petrova, T.V., Jeltsch, M., Jackson, D.G., Talikka, M., Rauvala, H., et al. (2004). Vascular endothelial growth factor C is required for sprouting of the first lymphatic vessels from embryonic veins. Nat. Immunol. *5*, 74–80.

Kulkarni, R.M., Greenberg, J.M., and Akeson, A.L. (2009). NFATc1 regulates lymphatic endothelial development. Mech. Dev. *126*, 350–365.

Kumai, M., Nishii, K., Nakamura, K., Takeda, N., Suzuki, M., and Shibata, Y. (2000). Loss of connexin45 causes a cushion defect in early cardiogenesis. Development *127*, 3501–3512.

Lehr, H.A., Leunig, M., Menger, M.D., Nolte, D., and Messmer, K. (1993). Dorsal skinfold chamber technique for intravital microscopy in nude mice. Am. J. Pathol. *143*, 1055–1062.

Mäkinen, T., Adams, R.H., Bailey, J., Lu, Q., Ziemiecki, A., Alitalo, K., Klein, R., and Wilkinson, G.A. (2005). PDZ interaction site in ephrinB2 is required for the remodeling of lymphatic vasculature. Genes Dev. *19*, 397–410.

May, S.R., Stewart, N.J., Chang, W., and Peterson, A.S. (2004). A Titin mutation defines roles for circulation in endothelial morphogenesis. Dev. Biol. *270*, 31–46.

Mellor, R.H., Brice, G., Stanton, A.W., French, J., Smith, A., Jeffery, S., Levick, J.R., Burnand, K.G., and Mortimer, P.S.; Lymphoedema Research Consortium. (2007). Mutations in FOXC2 are strongly associated with primary valve failure in veins of the lower limb. Circulation *115*, 1912–1920.

Ng, C.P., Helm, C.L., and Swartz, M.A. (2004). Interstitial flow differentially stimulates blood and lymphatic endothelial cell morphogenesis in vitro. Microvasc. Res. *68*, 258–264.

Norrmén, C., Ivanov, K.I., Cheng, J., Zangger, N., Delorenzi, M., Jaquet, M., Miura, N., Puolakkainen, P., Horsley, V., Hu, J., et al. (2009). FOXC2 controls formation and maturation of lymphatic collecting vessels through cooperation with NFATc1. J. Cell Biol. *185*, 439–457.

Petrova, T.V., Mäkinen, T., Mäkelä, T.P., Saarela, J., Virtanen, I., Ferrell, R.E., Finegold, D.N., Kerjaschki, D., Ylä-Herttuala, S., and Alitalo, K. (2002). Lymphatic endothelial reprogramming of vascular endothelial cells by the Prox-1 homeobox transcription factor. EMBO J. *21*, 4593–4599.

Petrova, T.V., Karpanen, T., Norrmén, C., Mellor, R., Tamakoshi, T., Finegold, D., Ferrell, R., Kerjaschki, D., Mortimer, P., Ylä-Herttuala, S., et al. (2004). Defective valves and abnormal mural cell recruitment underlie lymphatic vascular failure in lymphedema distichiasis. Nat. Med. *10*, 974–981.

Ringelmann, B., Röder, C., Hallmann, R., Maley, M., Davies, M., Grounds, M., and Sorokin, L. (1999). Expression of laminin alpha1, alpha2, alpha4, and alpha5 chains, fibronectin, and tenascin-C in skeletal muscle of dystrophic 129ReJ dy/dy mice. Exp. Cell Res. *246*, 165–182.

Rockson, S.G. (2008). Secondary lymphedema: is it a primary disease? Lymphat. Res. Biol. *6*, 63–64.

Saaristo, A., Veikkola, T., Tammela, T., Enholm, B., Karkkainen, M.J., Pajusola, K., Bueler, H., Ylä-Herttuala, S., and Alitalo, K. (2002). Lymphangiogenic gene therapy with minimal blood vascular side effects. J. Exp. Med. *196*, 719–730.

Schweighofer, B., Testori, J., Sturtzel, C., Sattler, S., Mayer, H., Wagner, O., Bilban, M., and Hofer, E. (2009). The VEGF-induced transcriptional response comprises gene clusters at the crossroad of angiogenesis and inflammation. Thromb. Haemost. *102*, 544–554.

Simon, A.M., and McWhorter, A.R. (2002). Vascular abnormalities in mice lacking the endothelial gap junction proteins connexin37 and connexin40. Dev. Biol. *251*, 206–220.

Simon, A.M., Goodenough, D.A., Li, E., and Paul, D.L. (1997). Female infertility in mice lacking connexin 37. Nature *385*, 525–529.

Srinivasan, R.S., and Oliver, G. (2011). Prox1 dosage controls the number of lymphatic endothelial cell progenitors and the formation of the lymphovenous valves. Genes Dev. *25*, 2187–2197.

Tarbell, J.M., and Ebong, E.E. (2008). The endothelial glycocalyx: a mechano-sensor and -transducer. Sci. Signal. *1*, pt8.

Tzima, E., Irani-Tehrani, M., Kiosses, W.B., Dejana, E., Schultz, D.A., Engelhardt, B., Cao, G., DeLisser, H., and Schwartz, M.A. (2005). A mechanosensory complex that mediates the endothelial cell response to fluid shear stress. Nature *437*, 426–431.

Vermot, J., Forouhar, A.S., Liebling, M., Wu, D., Plummer, D., Gharib, M., and Fraser, S.E. (2009). Reversing blood flows act through klf2a to ensure normal valvulogenesis in the developing heart. PLoS Biol. *7*, e1000246.

Wang, Y., Nakayama, M., Pitulescu, M.E., Schmidt, T.S., Bochenek, M.L., Sakakibara, A., Adams, S., Davy, A., Deutsch, U., Lüthi, U., et al. (2010). Ephrin-B2 controls VEGF-induced angiogenesis and lymphangiogenesis. Nature *465*, 483–486.

Wei, C.J., Xu, X., and Lo, C.W. (2004). Connexins and cell signaling in development and disease. Annu. Rev. Cell Dev. Biol. *20*, 811–838.

Wigle, J.T., and Oliver, G. (1999). Prox1 function is required for the development of the murine lymphatic system. Cell *98*, 769–778.

Wong, C.W., Christen, T., Roth, I., Chadjichristos, C.E., Derouette, J.P., Foglia, B.F., Chanson, M., Goodenough, D.A., and Kwak, B.R. (2006). Connexin37 protects against atherosclerosis by regulating monocyte adhesion. Nat. Med. *12*, 950–954.

Wu, H., Peisley, A., Graef, I.A., and Crabtree, G.R. (2007). NFAT signaling and the invention of vertebrates. Trends Cell Biol. *17*, 251–260.

Xu, Y., Yuan, L., Mak, J., Pardanaud, L., Caunt, M., Kasman, I., Larrivée, B., Del Toro, R., Suchting, S., Medvinsky, A., et al. (2010). Neuropilin-2 mediates VEGF-C-induced lymphatic sprouting together with VEGFR3. J. Cell Biol. *188*, 115–130.

Yoshimatsu, Y., Yamazaki, T., Mihira, H., Itoh, T., Suehiro, J., Yuki, K., Harada, K., Morikawa, M., Iwata, C., Minami, T., et al. (2011). Ets family members induce lymphangiogenesis through physical and functional interaction with Prox1. J. Cell Sci. *124*, 2753–2762.

Zaichuk, T.A., Shroff, E.H., Emmanuel, R., Filleur, S., Nelius, T., and Volpert, O.V. (2004). Nuclear factor of activated T cells balances angiogenesis activation and inhibition. J. Exp. Med. *199*, 1513–1522.

Zawieja, D.C. (2009). Contractile physiology of lymphatics. Lymphat. Res. Biol. *7*, 87–96.

Zeini, M., Hang, C.T., Lehrer-Graiwer, J., Dao, T., Zhou, B., and Chang, C.P. (2009). Spatial and temporal regulation of coronary vessel formation by calcineurin-NFAT signaling. Development *136*, 3335–3345.

Zeng, H., Chattarji, S., Barbarosie, M., Rondi-Reig, L., Philpot, B.D., Miyakawa, T., Bear, M.F., and Tonegawa, S. (2001). Forebrain-specific calcineurin knockout selectively impairs bidirectional synaptic plasticity and working/episodic-like memory. Cell *107*, 617–629.